# Model Theory and Analytical Solutions for Large Water Waves due to Landslides

C.B. Harbitz G. Pedersen
Department of Mathematics, Mechanics Division,
University of Oslo,
P.O.Box 1053 Blindern, 0316 OSLO 3, Norway

March 23,1992

**Abstract**

A mathematical model for simulation of large water waves due to landslides, including a numerical solution procedure, is described. A theory for estimation of run-up heights is presented, as well as simple, analytical solutions for wave excitation by slides.

# 1 Introductory remarks

This report contains elements of basic theory for simulation of slide generated water waves. Sections 2 and 3 describes a mathematical model and a numerical solution procedure applicable in the slide area and for the wave propagation in open sea regions. Sec.4 describes in detail the slide model, while sec.5 presents a theory for estimation of run-up heights at the shores. Finally we present a simple, analytical solution for wave excitation by slides.

# 2 Hydrodynamic equations

Waves generated by slides can often be classified as long waves. In other words most of the energy that is transferred from the slide to water motion is distributed on waves with typical wave-length, $\lambda$, which is much larger than the characteristic water depth, $h_0$. From the assumption $h_0/\lambda \ll 1$ it may be deduced that the pressure is approximately hydrostatic and that the vertical variations of the horizontal velocity are small. We will also assume that the characteristic amplitude of the waves, $a$, is much less than $h_0$. On basis of these assumptions we may derive the linearized shallow water equations (see Wu, 1981, Pedersen, 1989). Estimates of run-up heights on gentle beach slopes can also be found on basis of linear wave theory, as shown in sec.5.

The equations are formulated in a Cartesian coordinate system with horizontal axes, $Ox$ and $Oy$ in the undisturbed water level and the vertical axis, $Oz$, pointing upwards. The fluid is confined to $-h < z < \eta$ where $h$ is the depth referred to the datum $z = 0$, $\eta$ the water surface displacement and we denote the total water depth by $H = h + \eta$. Since the slide introduces bathymetric changes, $h$ will be a function of time ($t$). Mass conservation in a vertical fluid column leads to a continuity equation of the form:

$$\frac{\partial H}{\partial t} \equiv \frac{\partial \eta}{\partial t} + \frac{\partial h}{\partial t} = -\nabla \cdot \vec{Q} \tag{1}$$

where $\vec{Q}$ is the vertically integrated volume flux density and $\nabla\cdot$ denote the horizontal divergence operator. In terms of the averaged horizontal velocity, $\vec{u} = u\vec{i} + v\vec{j}$, where $\vec{i}$ and $\vec{j}$ denote the unit vectors in the $x$- and $y$-directions

respectively, the volume flux density can be approximated by:

$$\vec{Q} = h\vec{u} \tag{2}$$

and by substitution in eq.(1)

$$\frac{\partial H}{\partial t} = -\nabla \cdot (h\vec{u}) \tag{3}$$

We note that while eq.(1) is an exact form of the continuity equation, the use of eq.(2) introduces relative errors of order $a/h_0$ in eq.(3).

Based on the assumptions above the momentum equation becomes:

$$\frac{\partial \vec{u}}{\partial t} = -g\nabla\eta + \frac{\vec{\tau}}{\rho h} \tag{4}$$

where $g$ is the acceleration of gravity, $\rho$ is the density of the fluid and $\vec{\tau}$ is the bottom shear stress. Eq.(4) inherits relative errors of order $a/h_0$ as well as order $(h_0/\lambda)^2$.

# 3 Numerical solution of the linearized shallow water equations

The numerical approximation to a parameter $f$ at a grid-point with coordinates $(\beta\Delta x,\ \gamma\Delta y,\ \kappa\Delta t)$ where $\Delta x$, $\Delta y$ and $\Delta t$ are the grid increments, is denoted by $f^{\kappa}_{\beta,\gamma}$. In order to make the difference equations more readable we introduce the symmetric difference operator, $\delta_x$, and the midpoint average operator, $^{-x}$, by:

$$\delta_x f^{(\kappa)}_{\beta,\gamma} = \frac{1}{\Delta x}(f^{(\kappa)}_{\beta+\frac{1}{2},\gamma} - f^{(\kappa)}_{\beta-\frac{1}{2},\gamma}) \qquad (\overline{f}^{x})^{(\kappa)}_{\beta,\gamma} = \frac{1}{2}(f^{(\kappa)}_{\beta-\frac{1}{2},\gamma} + f^{(\kappa)}_{\beta+\frac{1}{2},\gamma}) \tag{5}$$

Difference and average operators with respect to the other coordinates $y$ and $t$ are defined correspondingly. We note that all combinations of these operators are commutative. To abbreviate the expressions further we also group terms of identical indices inside square brackets, leaving the super- and subscripts outside the bracket.

The eqs.(3) and (4) are discretized on a grid that is staggered both in time and space. Fig.1 shows the spatial distribution of the nodes which is

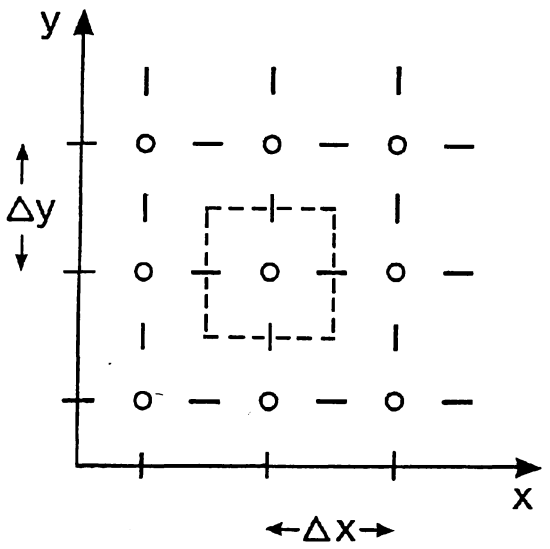


Figure 1: The spatial distribution of grid points.
o: Locations of $\eta$-points, —: locations of $u$-points,
| : locations of $v$-points, – –: boundaries of one grid cell.

often referred to as the Arakawa C grid (Mesinger and Arakawa, 1976). The discrete quantities are denoted by:

$$\eta^{\kappa}_{\beta,\gamma}\ ,\ u^{\kappa+\frac{1}{2}}_{\beta+\frac{1}{2},\gamma}\ ,\ v^{\kappa+\frac{1}{2}}_{\beta,\gamma+\frac{1}{2}}\ ,\ h^{\kappa}_{\beta,\gamma} \tag{6}$$

A finite difference version of eq.(3) reads:

$$[\delta_t\eta = -\delta_t h - \delta_x(\overline{h}^x u) - \delta_y(\overline{h}^y v)]^{\kappa+\frac{1}{2}}_{\beta,\gamma} \tag{7}$$

Eq.(7) assures volume conservation.

Predictor values for the velocity components $u^{\kappa+\frac{1}{2}}_{\beta+\frac{1}{2},\gamma}$ and $v^{\kappa+\frac{1}{2}}_{\beta,\gamma+\frac{1}{2}}$ are found from discretization of the components of the momentum equation (4) with $\vec{\tau}$ omitted:

$$[\delta_t u = -g\delta_x\eta]^{\kappa}_{\beta+\frac{1}{2},\gamma} \tag{8}$$

$$[\delta_t v = -g\delta_y\eta]^{\kappa}_{\beta,\gamma+\frac{1}{2}} \tag{9}$$

Subsequently corrected values for the velocity components are obtained by the implementation of $\vec{\tau}$, adding the terms $[\tau_x\Delta t/(\rho\overline{h}^x)]^{\kappa+\frac{1}{2}}_{\beta+\frac{1}{2},\gamma}$ and $[\tau_y\Delta t/(\rho\overline{h}^y)]^{\kappa+\frac{1}{2}}_{\beta,\gamma+\frac{1}{2}}$ to the predictor values of $u^{\kappa+\frac{1}{2}}_{\beta+\frac{1}{2},\gamma}$ and $v^{\kappa+\frac{1}{2}}_{\beta,\gamma+\frac{1}{2}}$ respectively. The explicit expression for $\vec{\tau} = \tau_x\vec{i} + \tau_y\vec{j}$ is given by eq.(18).

Eqs.(7) through (9) and the implementation of $\vec{\tau}$ define an explicit finite difference method of second order accuracy for which $\eta$ and $\vec{u}$ are evaluated at adjacent half time steps.

A rigid impermeable wall is represented by a sequence of line segments parallel to the axes. Each segment passes through nodes for the corresponding normal velocity component which is set to zero. This representation is accurate only to the first order in the grid increments and may in some cases give rise to spurious trapping effects (see Pedersen, 1986). Still, such boundaries are extensively used in models of the ocean and lakes because of their simplicity. A slide penetrating the water surface at a shore gives a non-zero normal flux at the boundary. Additional complications will arise from the fact that the shore line under such circumstances must be regarded as time dependent.

A grid cell is defined as the volume element circumvented by straight lines normal to the velocity directions in four velocity points around one point of surface elevation, fig.1. When the motion of the slide causes the depth in a grid cell to become negative (i.e. $h^{\kappa+1}_{\beta,\gamma} < 0$), the shore line is moved to the seaside of this cell. This is accomplished by setting the velocities along the line segments representing the new shore line equal to zero. The last calculated fluid volume in the cell, defined by

$$[V = \Delta x \Delta y(\eta + h)]^{\kappa}_{\beta,\gamma} \tag{10}$$

is spread equally over cells which have boundaries in common with the one drained, and still have a positive depth (i.e. $h^{\kappa+1}_{\beta,\gamma} > 0$), fig.2. Thus the total fluid volume is kept constant.

The time increment $\Delta t$ is determined by the Courant Friedrich Levy (CFL) stability criterion

$$\Delta t \leq (g h_{max}(1/\Delta x^2 + 1/\Delta y^2))^{-\frac{1}{2}} \tag{11}$$

If the slide velocity is so large that the slide moves more than one grid distance per time step, a reduced time increment is used during the slide event to avoid this. Reducing the time step this way do not introduce any significant numerical damping.

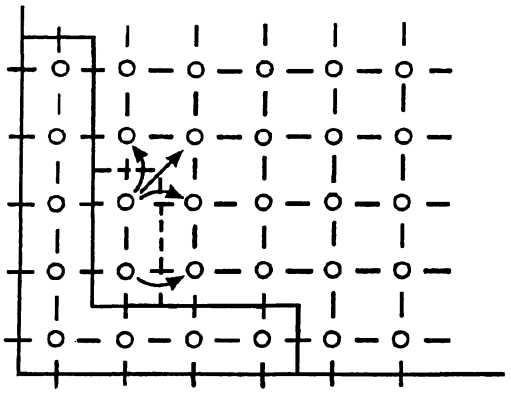

Figure 2: Distribution of fluid volume from grid cells with negative depth.
——: Line segments along the shore line at time $t = \kappa\Delta t$,
$- -$: line segments along the shore line at time $t = (\kappa + 1)\Delta t$,
$\longrightarrow$ : Indication of how the fluid volume is distributed.

# 4 The slide model

Energy transfer from the slide mass to the water is clearly a very complicated process which is impossible to model in detail. Firstly the composition of the slide may vary over a wide range from large blocks to fine particles. In the former case water will flow in between the blocks and each component will experience a resistance from viscous drag, form drag and added mass. The slide will also loose energy because of collisions and friction between the slide particles and because of the bottom friction. Secondly the slide characteristics may change considerably during the slide process; blocks may be crushed, mass may be released or deposited along the sea bed and water may be admitted into the total slide mass.

The process of water wave generation by slides may be controlled by the global characteristics of the slide. We shall therefore focus only on two important large scale energy transfer mechanisms; the total water displacement and the shear stress acting between the slide masses and the fluid. These effects are easily parameterized by the shallow water equations.

The total water displacement is determined by the aggregated displacement thickness of the slide. The slide will therefore be described as one body

with a prescribed motion. This corresponds to a time dependent water depth

$$h(x,y,t) = h_r(x,y) - h_s(x - x_s(t), y - y_s(t)) \tag{12}$$

where $h_r(x,y)$ represents the rigid sea floor, and $h_s$ describes the water displacement by the slide body. By assuming a simple functional relation for the slide retardation in water, the coordinates $(x_s(t), y_s(t))$ defined by

$$\left.\begin{aligned} x_s &= x_0 + (R\sin\tfrac{\pi t}{2T})\cos\varphi \\ y_s &= y_0 + (R\sin\tfrac{\pi t}{2T})\sin\varphi \end{aligned}\right\} \quad 0 < t < T$$

$$\left.\begin{aligned} x_s &= x_0 + R\cos\varphi \\ y_s &= y_0 + R\sin\varphi \end{aligned}\right\} \quad t \geq T \tag{13}$$

specify the motion of the slide. $\varphi$ is the angle between the propagation direction of the slide and the $x$-axis. $(x_0, y_0)$ is the position of the front of the slide at $t = 0.0$ s. $R$ is the total horizontal displacement during the time interval $T$. We shall refer to $R$ as the retardation distance and to $T$ as the running time of the slide. The velocity of the slide at the time it starts to penetrate the water surface ($t = 0.0$ s) is $U_0$ and from eq.(13) we have

$$T = \frac{\pi}{2}\frac{R}{U_0} \tag{14}$$

The velocity $U_0$ may be determined from the "Perla slide model" (Perla et al., 1980) based on estimates of slide and terrain parameters. $R$ will depend on the maximum kinetic energy of the slide, $E_s = \frac{1}{2}M_s U_0^2$, where $M_s$ is the mass of the slide. However, this functional relationship is unknown. An estimate of $R$ is therefore found simply by assuming that the slide will stop at a well defined breaking point along the depth profile.

The shape of the slide is represented by a box form of length $L$, width $B$ and maximum thickness $\Delta h$. To avoid sharp gradients in $h$, the edges of the box form are smoothed over a distance equal to $B$ along both sides and in the front by an exponential function of the form

$$h_s = \begin{cases} \Delta h \exp\left(-(2\frac{y'}{B})^4\right) & -(L+B) \leq x' < -B \\ \Delta h \exp\left(-(2\frac{x'+B}{B})^4 - (2\frac{y'}{B})^4\right) & -B \leq x' < 0 \end{cases} \tag{15}$$

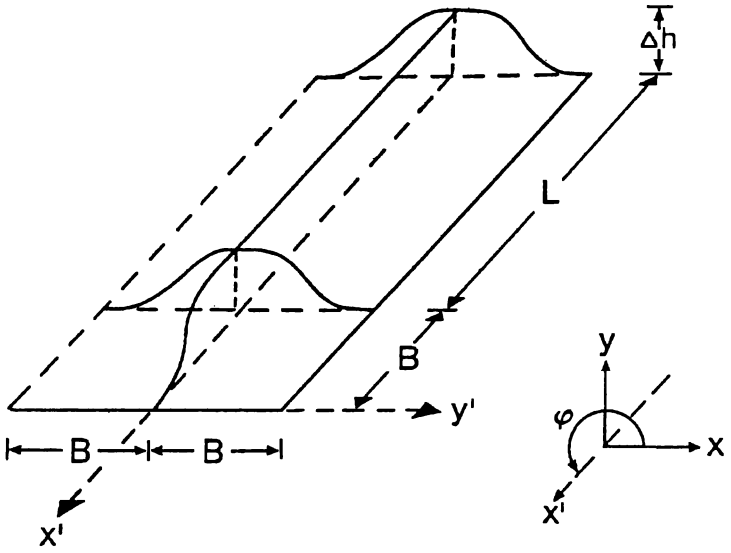


Figure 3: Sketch of slide body with characteristic parameters.
Thickness $\Delta h$, width $B$ and length $L$, volume $V_s = 0.90B\Delta h(L + 0.46B)$.

where

$$\begin{aligned} x' &= (x - x_s)\cos\varphi + (y - y_s)\sin\varphi \\ y' &= -(x - x_s)\sin\varphi + (y - y_s)\cos\varphi \end{aligned}$$

The $x'$-axis is directed along the direction of the slide motion, and the $y'$-axis in the transverse direction, with the origin in the front of the slide, fig.3.

The width of the slide, $B$, constitutes the width of that part of the box which is thicker than $0.37 \cdot \Delta h$. With this definition of $h_s$ the slide volume $V_s$ is

$$V_s = 0.90B\Delta h(L + 0.46B) \tag{16}$$

where the factors 0.90 and 0.46 arises due to the smoothening. The actual shape of the slide is sketched in fig.3. To ensure that the whole slide volume enters the water, we will choose $R = L + B$.

The slide model above may also be used for slides released under water. In this case eq.(13) is modified to

$$\left.\begin{aligned} x_s &= x_0 + \{\tfrac{1}{2}R(1 - \cos\tfrac{\pi t}{T})\}\cos\varphi \\ y_s &= y_0 + \{\tfrac{1}{2}R(1 - \cos\tfrac{\pi t}{T})\}\sin\varphi \end{aligned}\right\} \quad 0 < t < T$$

$$\left.\begin{aligned} x_s &= x_0 + R\cos\varphi \\ y_s &= y_0 + R\sin\varphi \end{aligned}\right\} \quad t \geq T \tag{17}$$

to allow for zero initial velocity of the slide mass. The volume, eq.(16), will be increased due to smoothening in the rear end as well, and we will impose no simple connection between $R$ and the slide parameters.

The bottom shear stress acting on the water is expressed by

$$\vec{\tau} = \frac{1}{2} c_D \rho [(\dot{x}_s - u)^2 + (\dot{y}_s - v)^2]^{\frac{1}{2}} \; [(\dot{x}_s - u)\vec{i} + (\dot{y}_s - v)\vec{j}] \qquad (18)$$

where $c_D$ is the drag coefficient (the dot denotes differentiating with respect to $t$). For most slides we have $\mid \dot{x}_s\vec{i} + \dot{y}_s\vec{j} \mid >> \mid \vec{u} \mid$, and the fluid velocity may be neglected in eq.(18).

# 5 Theory for estimation of run-up heights

## 5.1 General considerations

The numerical model presented in sec.3 is primarily designed to handle generation and propagation of waves in the deeper regions of the fluid domain. At the shores the model hopefully provides an adequate representation of the reflected waves, but will generally not produce correct run-up heights. The major shortcomings and difficulties concerning run-up calculations can be listed as follows:

1. The grid is too coarse for a proper resolution of the beach topography.

2. Large scale roughness in shallow regions, due to vegetation, boulders, buildings etc., are not accounted for.

3. The model does not reproduce the freely moving shore line, but invokes a no-flux condition at some limiting depth.

4. The basic theory is linear, whereas the flow field near the shores must be expected to be substantially influenced by nonlinearity.

5. It is not a trivial task to extract the characteristics of the incident waves, due to reflection and interference. Hence, a straightforward calculation of the run-up height predictions based on the incident wave parameters becomes difficult.

6. Wave breaking is not taken into consideration neither in deep water nor in the run-up zone. Breaking is generally assumed to reduce wave heights as well as run-up heights.

In view of point 5, and to some extent point 1, we have preferred to develop run-up predictions from the surface elevation, $\eta_d$, at a reference depth $d$ near the shore, modelled by the methods described in the previous sections. As long as the length of the incident wave is large, point 1 and 2 above will probably be of minor importance. In earlier studies it has been demonstrated that linear theory often provides surprisingly good run-up values (see Gjevik and Pedersen, 1981). Therefore, point 4 is not necessarily crucial either. However, point 3 really implies that our model really corresponds to an incorrect physical reality, save the parts of the shore displaying steep slopes. We will therefore discuss this point in some detail. These considerations will be based on calculations for a simple geometry defined by depth function, $h(x)$, that equals a constant, $h_l$, for $x > x_l > 0$ and becomes zero for $x = 0$. The shore line, which runs parallel to the $y$-axis, is introduced either as a vertical wall at $x = x_r > 0$ or as a freely moving shore line around $x = x_r = 0$. As incident wave we choose a single periodic harmonic, that allows for simple analysis and may represent the actual waves in realistic bathymetries as least as well as any other simple wave form like solitons etc.

## 5.2 Analytical run-up calculations

For the incident and reflected waves in the region $x > x_l$ we may write respectively:

$$\left.\begin{aligned} \eta_{in} &= Ae^{i(k(x-x_l)+\ell y+\omega t)} \qquad A \in R \\ \eta_{ref} &= De^{i(-k(x-x_l)+\ell y+\omega t)} \qquad D \in C \end{aligned}\right\} \tag{19}$$

where $k$,$\ell$ and $\omega$ fulfills the dispersion relation and the real parts, only, have physical significance. For all $x$ we correspondingly write:

$$\eta = \zeta(x)e^{i(\ell y+\omega t)} \tag{20}$$

Assuming $\tau = 0$, eliminating $u$ and $v$ from eqs.(3) and (4) and finally inserting the expression (20) we arrive at the ordinary differential equation:

$$\frac{d}{dx}(gh\frac{d\zeta}{dx}) + (\omega^2 - \ell^2 gh)\zeta = 0 \tag{21}$$

From (19) we obtain as off shore boundary condition:

$$\frac{d\zeta}{dx} + ik\zeta = 2ikAe^{ik(x-x_l)} \tag{22}$$

which can be applied whenever $x \geq x_l$. We define $F(x; x_r)$ as the solution of eq.(21) that also fits the conditions $F(x_r; x_r) = 1$ and $dF(x_r; x_r)/dx = 0$ if $x_r > 0$. The first requirement suffices to determine $F$ uniquely if $x_r = 0$, due to the singularity of eq.(21). In terms of $F$ the solution for $\zeta$ becomes:

$$\zeta(x) = \frac{2ikA}{F'(x_l; x_r) + ikF(x_l; x_r)} F(x; x_r) \tag{23}$$

where $F'$ denotes the derivative of $F$. The maximum run-up height, $R_u$, becomes accordingly:

$$\frac{R_u}{A} = \frac{2k}{\sqrt{F'(x_l; x_r)^2 + k^2 F(x_l; x_r)^2}} \tag{24}$$

It is fairly easily realized that $R_u/A$ is a continuous function of $x_r$, also for $x_r = 0$. This implies that the solution of the "rigid wall problem" becomes a close approximation to the solution of the "true run-up problem" for small $x_r$. To prove the continuity of $R_u/A$ we start by stating that the general solution of eq.(21) is a linear combination of $F(x; 0)$ and another function, $G(x)$, that inherits a logarithmic singularity at $x = 0$, as can be shown by standard application of the Frobenius method. Thus, we may write $F(x; x_r) = \mu(x_r)F(x; 0) + \nu(x_r)G(x)$ where $\mu$ and $\nu$ are determined through the boundary conditions: $F(x_r; x_r) = 1$ and $F'(x_r; x_r) = 0$. This implies that $\nu/\mu$ tends to zero sufficiently fast for $F(x; x_r)$ to approach $F(x; 0)$ for all $x \geq x_r$ as $x_r \to 0$.

The solutions for the case $x_r = 0$ and a linear bottom profile, $h(x) = h_l x/x_l$ for $x < x_l$, is thoroughly discussed in Pedersen (1985). For this bottom topography $F$ may be expressed in terms of confluent hypergeometric functions, that may be derived from Bessel functions when $\ell = 0$. The latter case is analyzed for more general incident waves in Gjevik and Pedersen (1981).

## 5.3 Discrete run-up calculations

Even though the two boundary value problems are nicely related, additional difficulties may arise during the discretization. Most considerations concern-

ing accuracy and convergence of numerical methods of the present type, rely on Taylor series expansion. Unfortunately, the use of this expansion may be inappropriate in run-up calculations where $\Delta x$ is larger than or comparable to $x_r$, which equals the radius of convergence for $\zeta$ at $x = x_r$. We will thus analyze the discrete problem along the lines of the previous subsection.

We assume that the geometry is discretized with $u$-nodes at the boundary $x = x_r$. The arithmetics runs almost as for the analytical case. Again we assume (19), but this time $k$, $\ell$ and $\omega$ have to obey the numerical dispersion relation:

$$\tilde{\omega}^2 = gh_l(\tilde{k}^2 + \tilde{\ell}^2) \tag{25}$$

where

$$\tilde{k} = \frac{2}{\Delta x}\sin(\frac{k\Delta x}{2}) \qquad \tilde{\ell} = \frac{2}{\Delta y}\sin(\frac{\ell\Delta y}{2}) \qquad \tilde{\omega} = \frac{2}{\Delta t}\sin(\frac{\omega\Delta t}{2}) \tag{26}$$

The discrete analogue to (20) defines discrete values $\zeta_\beta$ which have to be determined. Elimination of velocities from the discrete eqs.(7), (8) and (9) followed by separation of variables (introduction of $\zeta$) yields in analogy to eq.(21):

$$[\delta_x(g\overline{h}^x\delta_x\zeta) + (\tilde{\omega}^2 - \tilde{\ell}^2 gh)\zeta = 0]_\beta \tag{27}$$

The off shore boundary condition now reads:

$$[\tilde{m}\delta_x\zeta + i\tilde{k}\overline{\zeta}^x]_{\beta+\frac{1}{2}} = 2i\tilde{m}\tilde{k}Ae^{ik(\beta\Delta x + x_r - x_l)} \tag{28}$$

where $\tilde{m} = \cos\frac{1}{2}k\Delta x$ and $(\beta - \frac{1}{2})\Delta x + x_r > x_l$. The position number $\beta = \frac{1}{2}$ corresponds to $x = x_r$. Accordingly $\zeta$ assumes integer indexes. When $x_r > 0$ the discrete $F$ is defined through:

$$[\delta_x F = 0]_{\frac{1}{2}} \qquad F_1 = 1 \tag{29}$$

where $F_0$ is introduced as a fictitious value. The analytical case $x_r = 0$ has a proper numerical counterpart only if $[\overline{h}^x]_{\frac{1}{2}} = 0$, which implies that the fictitious value $\zeta_0$ does not enter the difference equation (27). A unique solution for $F$ can then be obtained by requiring $F_1 = 1$ and solving the tridiagonal system (27). As a consequence the discrete method automatically reproduce the nonsingular solution for $F$. Defining $\zeta_1$ as $R_u^*$ we then find:

$$\frac{R_u^*}{A} = \frac{2\tilde{m}\tilde{k}}{\sqrt{[\tilde{m}^2(\delta_x F)^2 + \tilde{k}^2(\overline{F}^x)^2]_{\beta-\frac{1}{2}}}} \tag{30}$$

for some $\beta$ fulfilling $(\beta - \frac{1}{2})\Delta x + x_r > x_l$. A study of calculated solutions show that the discrete results generally are in excellent agreement with the analytical results in spite of the singularity at x=0.

## 5.4 Correction factors for run-up

The surface elevation $\eta_d$, at a reference depth $h = d$ near the shore, is extracted from results of the model described in the previous sections. For steep sections of the beach the maximum value of $\eta_d$ approximates the run-up height closely, while an estimation of a correction factor would be desirable elsewhere. We proceed as follows:

1. An average bottom slope, $\theta$, and an appropriate abyss depth, $h_l$, are estimated from the depth matrix. We then define a simplified geometry by a linear depth function for $x < x_l = h_l/\theta$.

2. One (or several) characteristic period(s) and angle(s) of incidence are extracted from time-series analysis and contour diagrams for $\eta$.

3. The method of sec.5.3 is applied to the simplified geometry and wave characteristics from point 2 to yield a ratio $\zeta_d/A$ at the point $h = d$. When $\zeta_d$ is identified with appropriate maximum values of $\eta_d$, we find an estimate on $A$.

4. Using the value of $A$ from the previous point and the techniques described in sec.5.2 and Gjevik and Pedersen (1981), we find a run-up height $R_u$.

The resulting expression for $R_u$ should give a reasonable approximation unless there are several nodes between $h = d$ and the beach, or a node is situated close to $h = d$.

# 6 A simple, analytical solution for wave excitation by slides

An analytical solution for a two-dimensional, idealized case is presented in order to study the influence of the governing parameters. We also obtain an

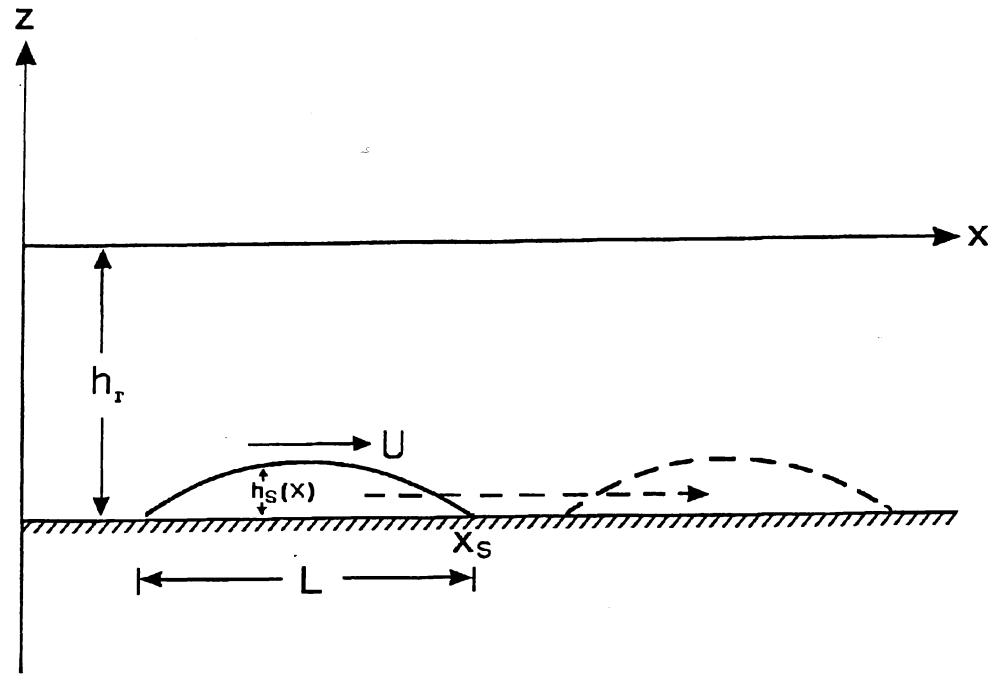


Figure 4: Slide motion in two-dimensional model.

expression for the relative importance of the effect of volume displacement versus the effect of shear stress on the interface between the fluid and the slide masses. The slide is assumed to maintain its initial shape and to move in the positive $x$-direction upon a horizontal sea-bed. It is at rest for $t \leq 0$, moves with constant velocity, $U$, for $0 < t < T$, and stops instantaneously at $t = T$. The length of the slide is $L$, the height from the sea bed to the undisturbed free surface is denoted by $h_r$ and the height of the slide, $h_s$, is assumed small when compared to $h_r$. A definition sketch of the slide is depicted in fig.4. Although the present slide model is extremely simple it still contains the essential parameters and the results obtained with this model may apply to realistic slide events as well.

Under the assumptions listed above the set of eqs.(3), (4), is easily solved by integration along characteristics or by combining free and forced wave solutions. For $t < T$ the solution consist of free waves, with phase speed $\pm c_0 = \pm\sqrt{gh_r}$ and a forced wave with speed $U$. The free and forced parts of the total solution are related by the initial conditions $\eta(x,0) = u(x,0) = 0$. At $t = T$ the forced solution gives rise to another family of free waves which are determined by patching $u$ and $\eta$. As a result, the wave system that propagates in the positive $x$-direction for $t > T$, can be described as the super position of two families of free waves which are phase shifted a distance $x_f = |c_0 - U|T$. The leading family corresponds to a surface elevation, whereas the trailing one corresponds to a depression. We may recognize

two contributions to the surface displacement, $\eta^\tau$ and $\eta^d$, due to the shear stress and the volume displacement respectively. We omit the details in the calculations and present only the right going solution for $t > T$:

$$\eta^d = \frac{F_r}{2|1-F_r|}(h_s(x-b-c_0t) - h_s(x-b+x_f-c_0t)) \tag{31}$$

$$\eta^\tau = \frac{1}{2\rho c_0^2|1-F_r|}(\Gamma(x-b-c_0t) - \Gamma(x-b+x_f-c_0t)) \tag{32}$$

where $b = max(\,(U-c_0)T,\,0\,)$ and the Froude number $F_r = U/c_0$. $\Gamma$ is a piecewise linear function of $x$ defined as:

$$\Gamma(x) = \begin{cases} 0 & x_0 < x \\ \tau\cdot(x_0-x) & x_0-L < x < x_0 \\ \tau L & x < x_0-L \end{cases} \tag{33}$$

where $x_0$ is the position of the front of the slide at $t = 0$. The solution is sketched in fig.5. For small $x_f$ the solution (31) may be approximated by:

$$\eta^d \approx -\frac{UT}{2}\frac{dh_s}{dx}(x-c_0t) \tag{34}$$

whereas $\eta^\tau$ has a constant value $\tau T/2\rho c_0$ for $x_0 - L < x < x_0 - x_f$. When $F_r \to 1$ we have $x_f \to 0$ and eq.(34) is valid exactly. We note that $\eta^\tau$ is discontinuous for this case.

Assuming $dh_s/dx \approx -2\Delta h/L$, where $\Delta h$ is the maximum value of $h_s$, we obtain from eq.(34) and eq. (33):

$$\eta^d_{max} \approx \frac{UT}{L}\Delta h \tag{35}$$

$$\eta^\tau_{max} \approx \frac{\tau T}{2\rho c_0} \tag{36}$$

For the other limiting case, $x_f > L$, we have

$$\eta^d_{max} \approx \frac{F_r}{2|1-F_r|}\Delta h = \frac{UT}{2x_f}\Delta h \tag{37}$$

$$\eta^\tau_{max} \approx \frac{\tau L}{2\rho c_0^2|1-F_r|} \tag{38}$$

Substituting for $\tau$ a one-dimensional version of eq.(18), with $\dot{x_s} = U$ and the fluid velocity neglected, we may in the latter case define a number:

$$\frac{\eta^\tau_{max}}{\eta^d_{max}} = c_D\frac{F_rL}{2\Delta h} \equiv \epsilon \tag{39}$$

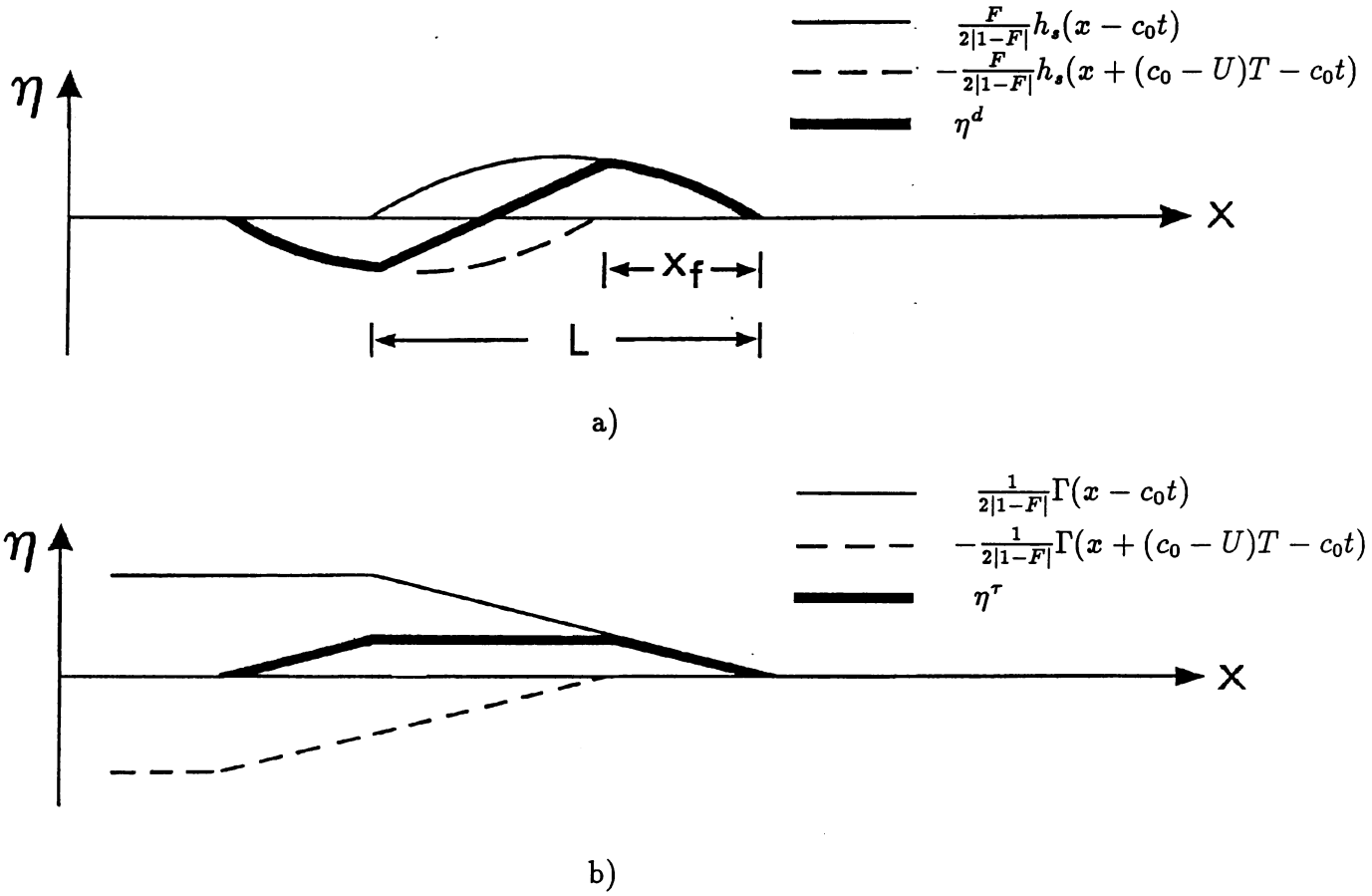


Figure 5: The surface elevation due to a: volume displacement and b: shear stress, for a typical slide.

which is a measure of the relative importance of volume displacement and bottom shear stress. For small $x_f$, we find that the corresponding ratio is $\frac{1}{2}\epsilon$. We note that the expression for $\epsilon$ is consistent with the natural assumption that a large horizontal extension of the slide favours the shear stress effects while the displacement becomes dominant for high slides. For slide events the travelling distance $UT = R$ can often be estimated. For a fixed $R$ the expressions for $\eta_{max}$ indicates that for nearly critical Froude numbers the largest $\eta^d$ will occur if $L \ll R$.

# References


Gjevik,B. and Pedersen,G. 1981: Run-up of Long Waves on an Inclined Plane. *Preprint Series, Dep. of Mathematics, University of Oslo* No. **2**.

Mesinger,F. and Arakawa,A. 1976: Numerical methods used in atmospheric models. *GARP, Publ. Ser. WMO* **17**, 64 pp.

Pedersen,G. 1985: Run-up of Periodic Waves on a Straight Beach. *Preprint Series, Dep. of Mathematics, University of Oslo* No. **2**.

Pedersen,G. 1986: On the Effects of Irregular Boundaries in Finite Difference Models. *Int. J. Numerical Methods in Fluids* Vol. **6**, pp. 497-505.

Pedersen, G. 1989: On the Numerical Solution of the Boussinesq equations. *Preprint Series, Dep. of Mathematics, University of Oslo* No. **1**.

Perla,R., Cheng,T.T. and McClung,D.M. 1980: A Two-parameter Model of Snow-avalanche Motion. *J. Glaciology* Vol. **26**, No. 24, pp.197-207.

Wu,T.Y. 1981: Long Waves in Ocean and Coastal Waters. *Proc. ASCE, J. Eng. Mech. Div.* **107**, EM3, pp.501-522.